



HAL
open science

On the installation of an in situ large-scale vertical SEALing (VSEAL) experiment on bentonite pellet-powder mixture

Nadia Mokni, Justo Cabrera, Frédéric Deleruyelle

► **To cite this version:**

Nadia Mokni, Justo Cabrera, Frédéric Deleruyelle. On the installation of an in situ large-scale vertical SEALing (VSEAL) experiment on bentonite pellet-powder mixture. *Journal of Rock Mechanics and Geotechnical Engineering*, 2023, 15 (9), pp.2388-2401. 10.1016/j.jrmge.2023.04.008 . irsn-04311582

HAL Id: irsn-04311582

<https://irsn.hal.science/irsn-04311582>

Submitted on 28 Nov 2023

HAL is a multi-disciplinary open access archive for the deposit and dissemination of scientific research documents, whether they are published or not. The documents may come from teaching and research institutions in France or abroad, or from public or private research centers.

L'archive ouverte pluridisciplinaire **HAL**, est destinée au dépôt et à la diffusion de documents scientifiques de niveau recherche, publiés ou non, émanant des établissements d'enseignement et de recherche français ou étrangers, des laboratoires publics ou privés.



Distributed under a Creative Commons Attribution - NonCommercial - NoDerivatives 4.0 International License

On the installation of an in situ large-scale Vertical SEALing (VSEAL) experiment on bentonite pellet/powder mixture

Nadia Mokni*, Justo Cabrera, Frédéric Deleruyelle

Institut de Radioprotection et de Sûreté Nucléaire (IRSN), PSE-ENV/SEDRE/LETIS, Fontenay-aux-Roses, 92260, France

Abstract: Recently, the Institute for Radiological protection and Nuclear Safety (IRSN) has launched VSEAL (Vertical SEALing) project to investigate the impact of gas migration on the long-term performance of bentonite based vertical sealing systems (VSS). The first VSEAL in situ test was emplaced in IRSN's Underground Research Laboratory (URL) in Tournemire (France) in 2019 and was equipped with 76 wired and wireless sensors. The test is still in progress, but the collected set of data provides already valuable information of the hydro-mechanical behavior of VSS during hydration. The swelling core consists of a mixture of high-density pellets and powder of MX80 bentonite in a ratio of 80/20 (in dry mass). An innovative method was adopted to drill a 1-m diameter and ~10-m deep shaft in order to minimize the rock perturbation at the sidewalls. Because a specific protocol was adopted to install the bentonite mixture together with a careful characterization of the core during construction, VSEAL 1 constitutes the unique in situ sealing test with a well-known initial structural distribution of the pellets and the powder. Some heterogeneities occurred within the experiment during the installation process: a damaged zone developed around the shaft walls due to the interruption of the installation operations caused by COVID19 lockdown in France; a technological gap with a variable thickness between the last pellets layer and the top confining lid and a heterogeneous distribution of the bentonite powder at some layers inducing large internal pellets voids close to the bentonite-rock interface. Artificially injected water volume, relative humidity, water content and swelling pressure in both radial and axial directions were monitored. Comparison of the results showed that the presence of installation-induced heterogeneities led to the generation of preferential flow paths that influenced the swelling pressure evolution at radial and axial directions.

Keywords: bentonite pellet-powder mixture; heterogeneities; technological gap; seals; in situ test

1. Introduction

Vertical sealing systems (VSS) (Surface-to-bottom seals) of a deep geological disposal, composed of bentonite-based materials, are one of the key elements for the safety of a facility such as the Cigéo project, since they would constitute the main potential pathway between the nuclear wastes and the biosphere. In the geological context of the French Cigéo project (Fig. 1), the upper layer of the bentonite vertical sealing material should be saturated in few years while total saturation of the core would need a few thousand years to be achieved (IRSN, 2014). This fast hydration leads to a rapid increase of water pressure in this zone, which should rapidly reach 30-40 bar. Over time and depending on the rate of gas production, gas reaches the VSS while the bentonite core is only partially saturated. Due to the host rock properties (calcareous Oxfordian), a very limited excavation damaged zone (EDZ) is expected around the shaft. Under these conditions, the partially saturated bentonite seal is likely to be solicited both by gas (from the bottom) and water pressures (from the top). Hence, a complete understanding of the VSS under hydraulic and gas solicitations is required for assessing its performance.

The transport of gases in clay-based buffer/sealing systems has been the subject of different international research programs during the last two decades. In bentonite, this process is controlled by the saturation history of the material (e.g. Horsmann et al., 1999; Harrington et al., 2003; Villar et al., 2012a; Cuss et al., 2014; Graham et al., 2016), which strongly affects its microstructural features (particularly the pore size distribution and the connectivity of the pore space). These changes in the pore network play an important role in the two-phase flow properties and in the initiation of localized pathways during the gas phase invasion. It is thus important to explore these gas migration properties under different saturation states that can be reached under varying water pressurisation rates.

A large proportion of the experimental research performed concerns laboratory tests of gas flow through fully saturated compacted specimens (Horseman et al., 1999; Harrington and

Horseman, 2003; Harrington et al., 2012a; Villar et al., 2012b; Graham et al., 2014, 2016; Namiki et al., 2014; Harrington et al., 2017; Carbonel et al., 2019; Gutiérrez-Rodrigo et al., 2021). Most of the results suggests that for bentonite-based mixtures with high sand content, transport occurs predominantly by visco-capillary two phase flow. For pure bentonite, gas migration occurs by the formation and propagation of dilatant pathways (e.g. Marshall, 2005; Graham et al., 2012; Ye et al., 2014). When the gas breakthrough pressure exceeds total stress, a mechanical interaction between the gas and the clay matrix begins leading to the generation of gas pathways.

Pre-existing pathways (EDZ, interfaces, and gaps) may also play an important role in gas migration process. Wang et al. (2103) and Saba et al. (2014) pointed out that at laboratory scale, the degree of swelling allowed by technological voids (gaps) has a significant influence on the HM behavior of compacted bentonite. At large scale, Mokni et al. (2016a) showed that technological gaps constituted preferential flow paths that accelerated water infiltration during the hydration of Sealex in situ tests. Gens et al. (2011) indicated that technological voids enhance the initial heterogeneity of clay barriers and seals. Mokni et al., (2016b) demonstrated that technological gaps and initial structural heterogeneities might result in a heterogenous distribution of bentonite dry density which might lead to remaining gradient after full saturation. Since gas transport is often a local phenomenon, these remaining low-density zones may act as preferential pathways for the migration of gas. Gas transport experiments involving bentonite in contact with other porous materials suggest that interfaces between the bentonite and other engineered components may serve also as preferential pathways for the gas flow. Although the role of laboratory tests is crucial in understanding gas migration processes through bentonite-based materials, uncertainties remain regarding representative boundary conditions for a given repository concept. Previous studies demonstrated that gas migration processes in bentonite-based materials are strongly dependent on the experimental configuration in terms of bentonite density, compaction procedure and mixture used, the stress state (swelling pressure), the

*Corresponding author. E-mail address: nadia.mokni@irsn.fr

hydration rate, the water saturation state and the role of pore water chemistry (pH properties), the local deformation undergone by the material, the gas injection regime (rapid/slow injection rates), and the role of internal pathways and external cell-mixture interfaces.

In order to understand the gas migration process in the bentonite buffer/seal system under repository-relevant conditions, in situ large-scale gas injection tests were undertaken in the last decades either in crystalline or Clay Underground Research Laboratories (URLs) (Sellin et al., 2006; Cuss et al., 2010, 2014; Vomvoris et al., 2011; Harrington et al., 2012b; de La Vaissière et al., 2014, 2015; Forge, 2014; Troullinos and Verstricht, 2015). Most of these tests were conducted on compacted bentonite-based materials. Gas injection testing was mostly performed after an artificial hydration period. In most cases, field testing data analysis evidenced that gas migration occurs principally by pathway propagation and dilatancy (Cuss et al., 2010, 2014). Although for some in situ tests, it turned out that the performance of the experiment is very sensitive to construction/field details such as the presence of technological gaps, interfaces or excavated damaged zones (Vomvoris et al., 2011; Troullinos and Verstricht, 2015).

Given the complex hydration scenario of the French VSS (fast hydration on the upper face by water flow from the Calcareous Oxfordian formation and slower hydration on the lateral surface by

water coming from the more impermeable Callovo-Oxfordian rock), gas might be trapped at the bottom of the seal, which will also be affected by gas generated by long-term metallic corrosion processes. In this context, the Institute for Radiological protection and Nuclear Safety (IRSN) has launched VSEAL project to investigate the impact of gas migration on the long-term performance of bentonite-based VSS. This project relies on two in situ experiments emplaced in IRSN's URL in Tournemire (South France) and small-scale tests conducted in laboratory. The VSEAL in situ experiments aim to (i) investigate the impact of gas migration during saturation of the bentonite vertical seal, (ii) study gas migration processes through the saturated bentonite core (preferential flow paths, role of interfaces).

The in situ tests are performed on MX80 highly compacted bentonite pellets and powder mixture (Pusch, 1979; Yong et al., 1986; Villar, 2008). This mixture is initially heterogeneous. The degree and distribution of heterogeneities will vary during the installation and hydration (Molinero et al., 2017, 2018; Mokni et al., 2019). Low-density zones can remain within the buffer mixture, potentially enhancing the transport of radionuclides during the long operating period. Indeed, a specific focus of VSEAL program is to investigate the role of installation-induced heterogeneities on the gas transport mechanisms.

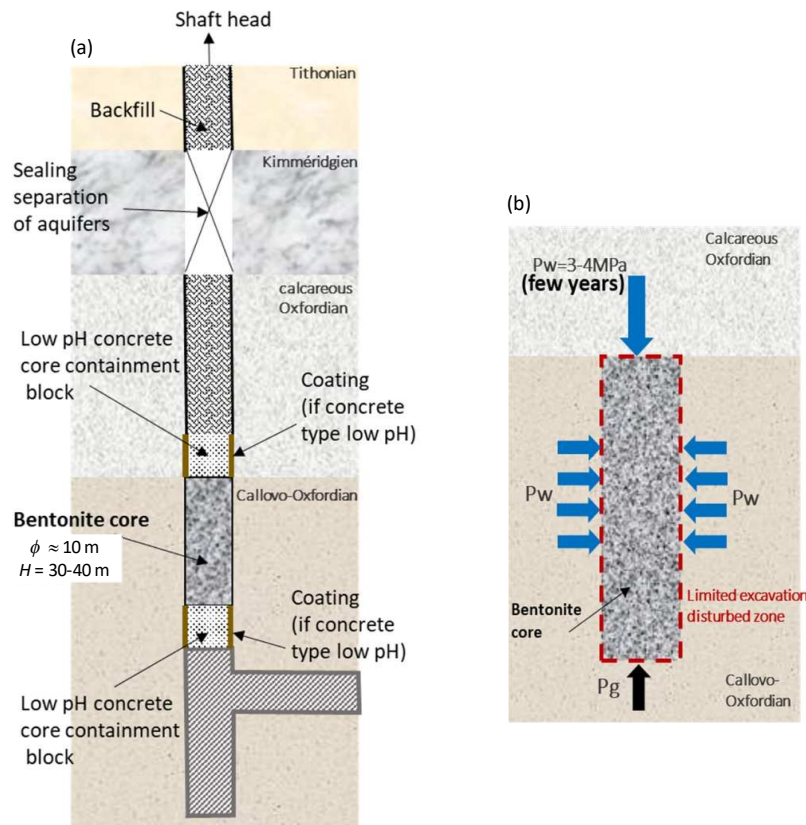


Fig. 1. (a) View of vertical sealing system in the French concept, and (b) Saturation scheme of the seal core. The diameter (ϕ) of the VSS in the future Cigéo facility is ~ 10 m. The height (H) is between 30 m and 40 m (Andra, 2021).

This paper aims at describing the design and installation of the first VSEAL in situ test, VSEAL 1. To begin with, the VSEAL experimental program is described. The installation phases including the drilling of the large diameter borehole are then detailed. Finally, the first experimental results obtained during the hydration stage are presented and compared.

2. VSEAL experimental program

The VSEAL project aims to study the impact of gas migration on the long-term performance of VSS. The VSEAL experimental program relies on two in situ experiments at a scale of 1/10 of the VSS (Fig. 1)

conducted in IRSN's Tournemire URL, located in a Mesozoic sedimentary basin on the western edge of the French Causses (southern part of France). These experiments aim at studying the vertical barrier's asymmetric hydration process and its consequences on gas migration at different hydraulic states.

Two vertical boreholes of 1 m in diameter will be drilled in the north_08 gallery (Fig. 2). Installation and drilling are based on the previous experience obtained from the SEALEX experiments (Mokni et al., 2016). Each experiment consists of a bentonite-based core mechanically confined at both ends, which represents a generic seal mock-up (1/10 VSS), except for the artificial saturation system.

The first in situ test VSEAL 1 will be a reference test, used to observe bentonite re-saturation without gas perturbation. However, a gas testing phase is foreseen after reaching full saturation. For the second in situ test VSEAL 2, gas will be injected from the bottom surface during the re-saturation phase to mimic the bottom gas pressure increase on the upper saturated layer of the VSS under in situ conditions.

For each VSEAL test, multiple pore pressure, total pressure, and relative humidity (*RH*) sensors will be installed within the bentonite core and at the bentonite-rock interface to follow swelling pressure evolution and water saturation. For VSEAL 1, various injection gas phases will be performed once the bentonite reaches full saturation. To avoid potential flow paths along cables and sensors within the bentonite core, wireless sensors have been preferred to classical wired sensors.

The installation phase of the reference test VSEAL 1 including the drilling phase was undertaken from September 2019 to August 2021. It must be noted that the installation work was interrupted several times due to COVID19 lockdown in France. The artificial hydration phase was launched in October 2021 and is currently on going. The installation of VSEAL 2 experiment started in February 2023. The drilling phase was undertaken in October 2022.

3. Test design and geometry

The general layout of VSEAL 1 in situ experiment is based on a swelling clay core composed of mixture MX80 bentonite pellets and powder (80/20 in dry mass) confined between two containers (lids) (Fig. 3). These elements are inserted in a vertical borehole excavated in Tournemire URL argillite. Borehole diameter was 1.005 m while the maximum reached depth was 9.6 m. The bentonite core was built between the depth of 5.72 m and 9.22 m, underneath the EDZ that is present around the gallery drift.

The shaft walls and the bentonite core were equipped by several sensors to follow the hydro-mechanical (HM) performance.

Water is injected from the top surface by means of injection lines connected to the top lid which will slowly saturate the upper part of the bentonite core. After reaching full saturation, gas will be injected from the bottom surface to observe the perturbation induced by gas. This will be done thanks to an inclined borehole, intersecting the main borehole at its bottom. Additional boreholes were drilled to extract the cables of the instrumentation installed at the rock/clay core.

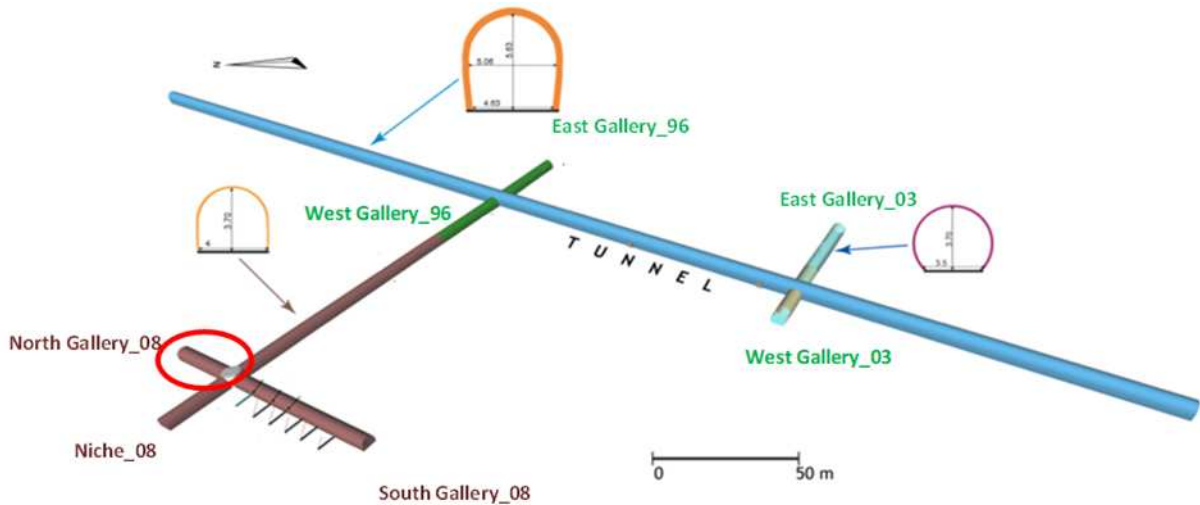


Fig. 1. View of Tournemire URL and the area where VSEAL in situ tests are installed.

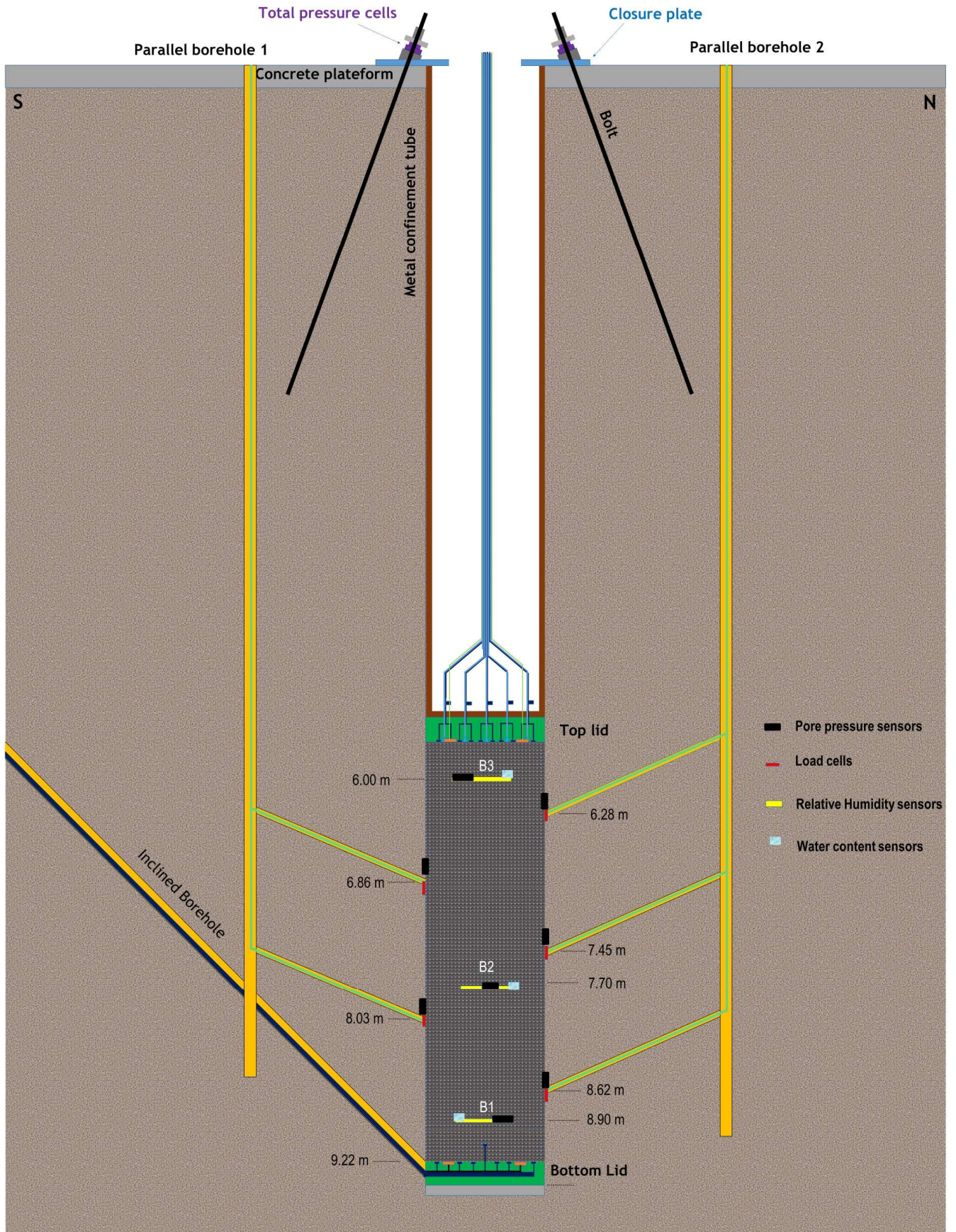


Fig. 3. General layout of VSEAL 1 in situ test

4. VSEAL 1 in situ test components

VSEAL 1 experiment is composed of four main components: (i) the bentonite-based core, (ii) the confinement system, (iii) the hydration and gas injection system, and (iv) intra-core and core-rock interface instrumentation.

4.1. Bentonite-based core

The investigated material is a mixture of pellets and powder of MX80 bentonite (Wyoming, USA) with a proportion of 80 pellets/20 powder in dry mass prepared at a dry density $\rho_d = 1.49 \text{ Mg/m}^3$ (DOPAS, 2016). According to the design requirement (Andra, 2016), bentonite-based seals behave as a hydraulic barrier that oppose the water circulation inside the structure. The material and its emplacement dry density should ensure a swelling pressure remaining within a range up to a maximum of 40 bar and a water permeability lower than 10^{-11} m/s .

The material has a high smectite content (80%) with some inclusions of non-clayey minerals (quartz – 4% of the total mass; muscovite – 4% of the total mass; pyrite – less than 1% of the total mass; and some elements of calcite). The cation exchange capacity (CEC) is 98 meq/100 g, with Na^+ as the major exchangeable cation. The liquid limit is 560%, the plastic limit is 62%, and the unit mass is 2.77 Mg/m^3 (Molinero et al., 2017). Pellets were industrially produced in Laviosa-MPC Company by instantaneously compacting a powder of MX80 bentonite in a mould of 0.032 m in diameter and 0.032 m in height (Laviosa Minerals). The fabrication was done at water content $w = 5\%-7\%$ and dry unit mass $\rho_d = 1.998\text{-}2.12 \text{ Mg/m}^3$. Pellets were received in packages of 25 kg and stored in Tournemire URL. The measured water content after a long storage period varies between 6.1% and 11.1%, indicating that package sealing was not efficient. The average water content value of the pellets is $w = 8.2\%$. The MX80 bentonite powder constituting the mixture was produced by crushing pellets. The produced powder grains present a diameter between 0.0008 m and 0.002 m (Molinero et al., 2017). Compared to the fabrication value of water content (between 5% and 7%), a value of 8.5% was found in the laboratory.

4.2. Confinement system

VSEAL 1 confinement system is composed of a bottom lid, a top lid, a confinement tube, and a closure plate (Fig. 3). The bottom lid rests on the bottom of the shaft, providing gas and water tightness as well as mechanical support to the bentonite core on top of it. Its mechanical structure consists basically of an external stainless-steel cylindrical body to withstand the weight of the buffer and upper structures, as well as the swelling pressure. This body comprises two circular plates on top and bottom, with a diameter of 0.98 m and a thickness of 0.02 m, and a side ring with a diameter of 0.098 m, a thickness of 0.02 m and a height of 0.17 m (Figs. 4 and 5). The ring has a side opening with a passthrough plate with fittings to allow the passthrough of gas injection lines from the inclined borehole to the injection points and the passthrough of cables from the sensors in the lid to the gallery (Fig. 5).

Inside the body, a welded grid of 12 vertical chambers made of carbon steel tube adds extra mechanical strength (Fig. 5a). In addition, four steel supports are welded to the lower plate to allow the installation of four total pressure cells through openings in the upper plate (Fig. 5a). Prior to the welding of the upper plate, the voids inside the lid are filled up almost to the top with resin to enhance the gas tightness and the mechanical strength of the lid (Fig. 5b). Then the upper plate is welded to the side ring. The filling up of the last void is completed through openings in the plate (Fig. 5c).

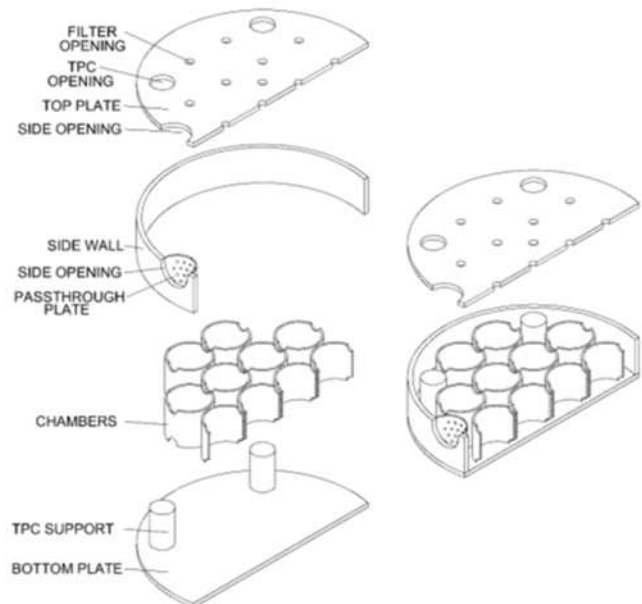


Fig. 4. Mechanical design of bottom lid.

The top lid rests on the top face of the bentonite core, providing gas and water tightness to the bentonite core, as well as mechanical confinement (Fig. 6). The top lid has the same mechanical structure as the bottom lid. It also comprises an inner grid of chambers made of tubes and an external stainless steel cylindrical body, but with a few differences in the lower plate: it has a thickness of 0.025 m; and a chamfer to house a soft rubber peripheral O-ring on top of the buffer. In addition, there is no side opening in the side wall, as all cables and lines pass through holes drilled in the top plate (Fig. 6). As for the bottom lid, four steel supports are welded to the lower plate to allow the installation of four total pressure cells through openings. The lid is constructed upside down, that is, with the lower plate on top, thus prior to the welding of said plate, the voids inside the lid are filled up almost to the top with the same resin used for the bottom lid (Fig. 6). Then the lower plate is welded to the side wall, and the filling up of the last void is completed through openings in the plate.

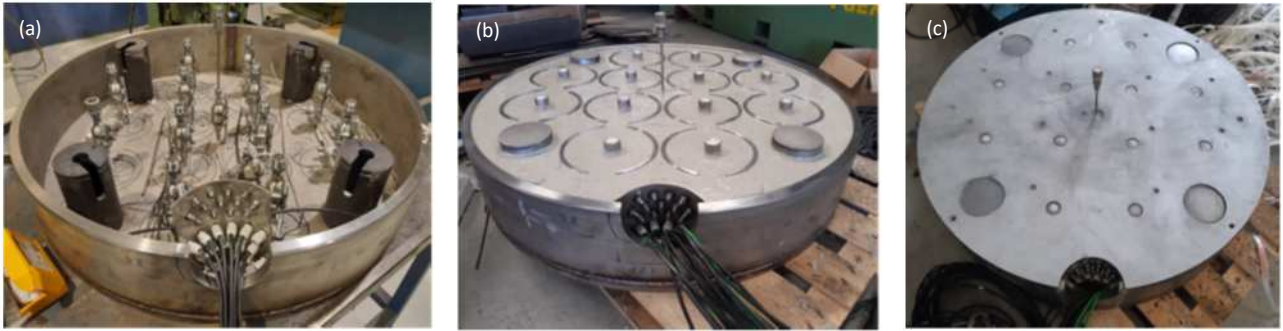


Fig. 5. Bottom lid: (a) Lid during assembling, (b) Lid after filling with resin, and (c) Lid after welding the top plate and sealing the upper voids with resin.



Fig. 6. View of top lid.

The central confinement tube provides mechanical confinement by transmitting the vertical swelling force exerted by the bentonite on the top lid to the external closure plate (Figs. 3 and 7). It measures 6 m in total, to exceed the shaft depth and provide enough length for adjustments on the top. The tube has been constructed in modular flanged pieces, each one consisting basically of a section of carbon steel tube with a diameter of 0.98 m and a thickness of 0.015 m. The tube is reinforced inside with horizontal rings made of bent 0.04 m U profile each half meter, and with 8 vertical nerves made of the same profile, connecting the rings.



Fig. 7. Confinement tube composed of four sections.

Finally, a circular plate on top of the tube closes the shaft. It consists of a 0.05 m-thick round plate measuring 1.8 m in diameter with a central round opening measuring 0.6 m in diameter to grant service access to the shaft (Fig. 8). It features 12 radial openings for 3 m-long anchoring bolts measuring 0.032 m in diameter, placed at a vertical angle of 20° to improve its strength against the vertical pushing force.



Fig. 8. View of the closure plate.

4.3. Hydration and gas injection systems

The main function of hydration is to ensure an inflow of water enabling saturation of the core from the top side during the testing period (10-15 years), without compromising the global tightness of the system. The gas injection system allows gas inflow at the bottom of the bentonite core and gas outflow at the top of the bentonite core. The hydration and gas injection systems are embedded into the top and bottom lid. Two series of filters are housed into the top lid surface to ensure water injection and gas outflow. A grid is welded on the surface of the lid (Fig. 9b). It is composed of several boxes to separate each filter series. The role of the grid is to help detecting the gas pathway. The first filter series is dedicated to perform a uniform water injection at the lid-bentonite core interface. Each filter is housed into the lid surface within one grid box (Fig. 9). A second series of filters ensure gas detection. In this case, each grid box houses 4 gas filters placed as shown in Fig. 9.

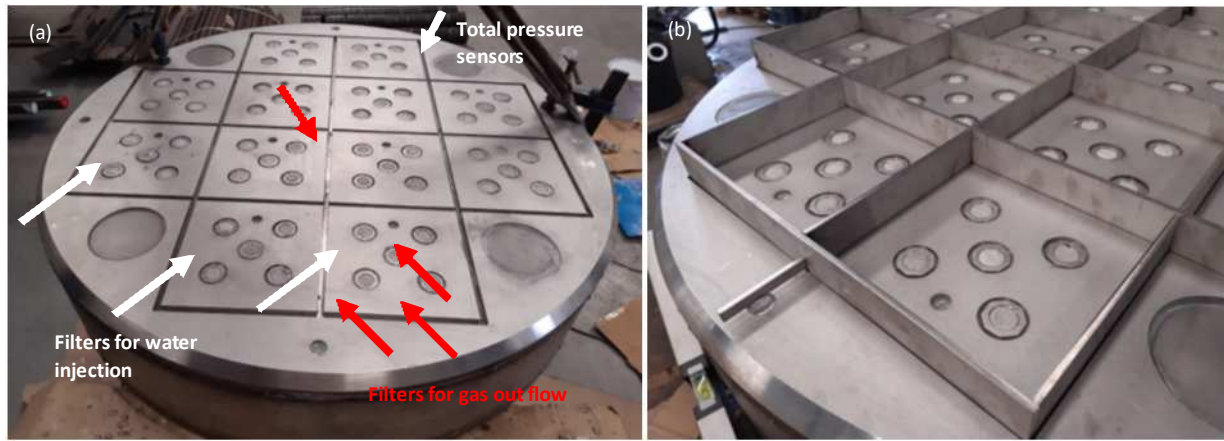


Fig. 9. Hydration and gas outflow systems in top lid: (a) Filters of water injection and gas outflow, and (b) Grid welded on the surface of the top lid.

For the bottom lid, gas injection is ensured also using a series of filters allowing performing a uniform gas injection at the lid-bentonite-core interface (Fig. 10). To allow a localised gas injection into the bentonite core, a filter measuring 0.015 m in diameter is housed into a needle made of a stainless-steel tube (Fig. 10).

The filters installed in the top and bottom lids are composed of a sintered porous metal and measures 0.025 m in diameter (Figs. 9 and 10) except of the needle like filter. Each filter is housed in holes in the lid plate and remains in contact with the bentonite through a geotextile disk installed on top. The water filters have a small pore size (4×10^{-5}) to prevent bentonite intrusion and ensure an easy water injection. The filters used for gas injection prevents water transfer (pore size of 2×10^{-7}) and avoid any water bypass.

4.4. Instrumentation

A total of 76 sensors were installed in VSEAL 1 in situ test. Eighteen wireless sensors were installed within the bentonite-based core to monitor pore pressure (6 PP sensors), relative humidity (6 RH sensors) and water content (6 WC sensors). The bentonite sensors are distributed in three sections located at different depths as shown in Figs. 3 and 11. The instrumented sections have been deployed to obtain a homogenous sensing field (Fig. 11).

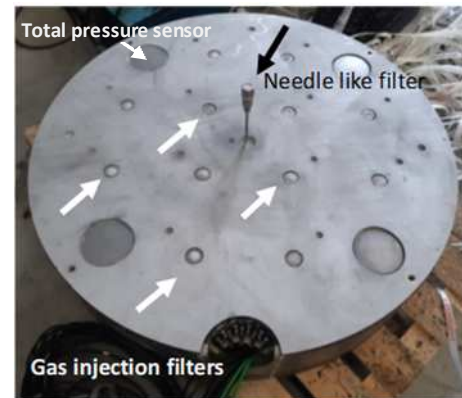


Fig. 10. View of gas injection filters in bottom lid and total pressure sensors.

In each section, the sensors are inscribed in a centred circumference measuring 0.25 m in diameter and placed horizontally trying to take just one layer of pellets. To minimize the perturbation caused by voids around the wireless system emitter (WSE) units in the same vertical profiles, each section is turned 90° from the previous one. To minimize potential preferential pathways, the cables connecting the sensors and the WSE units were surrounded by perforated pellets to stop any pathway along them (Fig. 12).

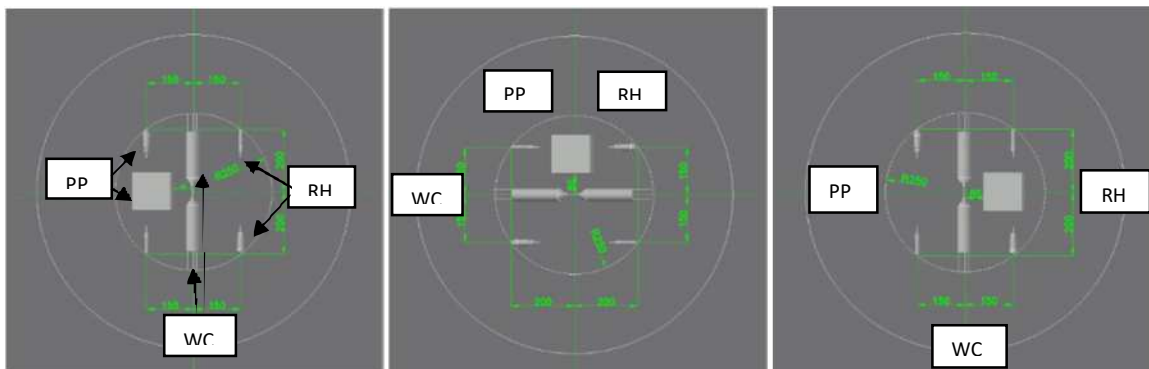


Fig. 11. View of the three instrumented sections installed within the bentonite core. Each section is turned 90° from the previous one.

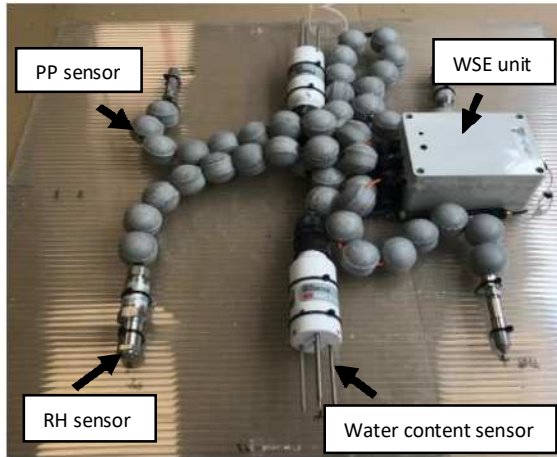


Fig. 12. View of a bentonite instrumented section with cables surrounded by perforated pellets.

To measure gas pressure during gas injection, the gas filters on the top and bottom lids are connected to 25 pressure sensors (12 on the top lid and 13 on the bottom lid). Eight total pressure sensors are installed on the metal plate (bottom for top lid and top for bottom lid) to measure the axial swelling pressure (Figs. 9 and 10). At the bentonite-rock interface, 10 wired sensors were distributed in 5 sections located at different depths to monitor pore pressure (5 sensors) and total pressure (TP) (5 sensors) (Fig. 13a). At each section, the wireless system receivers (WSRs) units together with PP and TP sensors were fully housed in recesses mechanised in the rock interface,

including slots to allow the passage of cables (Fig. 13b). The different instrumentation sections are summarized in Table 1.

Table 1. Instrumented sections and sensors.

Depth (m)	Section	Sensors name
-5.72	Top lid	PP-BT- i ($i = 1, 12$) TP-BT- i ($i = 1, 4$)
-6	Bentonite, B3	RH-B1-1, RH-B1-2 (relative humidity) WC-B1-1, WC-B1-2 (water content) PP-B1-1, PP-B1-2 (pore pressure)
-6.28	Rock R5	TP-R5 (total pressure) PP-R5
-6.86	Rock R4	TP-R5 (total pressure) PP-R5
7.45	Rock R3	TP-R5 (total pressure) PP-R5
-7.7	Bentonite B2	RH-B2-1, RH-B2-2 (relative humidity) W-B2-1, W-B2-2 (water content) PP-B2-1, PP-B2-2 (pore pressure)
-8.03	Rock R2	TP-R5 (total pressure) PP-R5
-8.62	Rock R1	TP-R5 (total pressure) PP-R5
-8.9	Bentonite B1	RH-B3-1, RH-B3-2 (relative humidity) W-B3-1, W-B3-2 (water content) PP-B3-1, PP-B3-2 (pore pressure)
-9.22	Bottom lid	PP-BB- i ($i = 1, 12$) TP-BB- i ($i = 1, 4$)

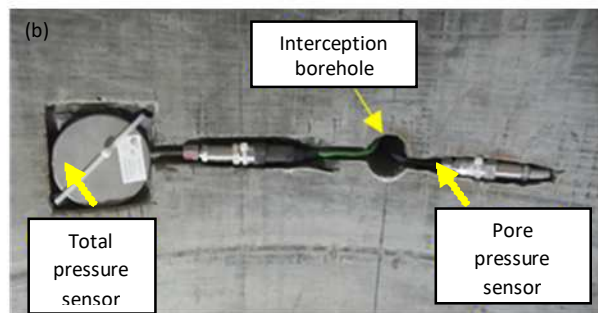
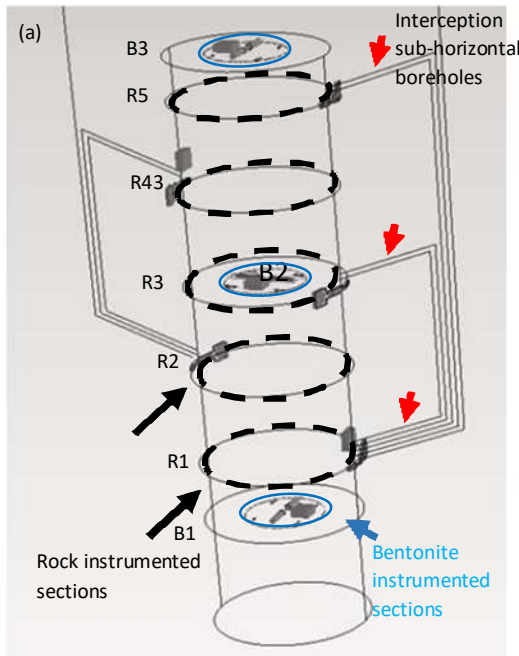


Fig. 13. (a) Rock sensor sections location and wiring, and (b) Rock sensor section: total pressure and pore pressure sensors inserted into slots mechanized in the rock interface.

In addition to these sensors, VSEAL 1 is equipped with 12 load cells that have been bolted to the closure plate to measure the axial pressure applied by the bentonite core on the central metal tube, together with three displacement sensors (Fig. 14).

The total pressure cells (EARTHSYSTEM CP-02-TO-10-R) and the pore pressure sensors (KELLER PA23SY) (Figs. 12 and 13b) were supplied with individual calibration certificates by the manufacturer. However, the functionality of all of them were tested in situ. The sensor selected to measure relative humidity and temperature is a tailored

system based on the commercially available Sensirion DHT75 model (Fig. 12) and the sensor selected to measure water content in the bentonite core is the well proven DELTAML3 TheraProbe sensor (Fig. 12). Finally, the sensor selected to measure the forces applied to the closure lid is the SISGEO model 0L205V0500T load cell, complemented with a suitable distribution plate and transmitter (Fig. 14). The displacement sensor placed at closure plate is ATEK LTM-50-A, which is based on potentiometric measure. Three sensors are installed in a 120° array with tailor-made mounting accessories (Fig. 14). Table 2 summarizes sensor types.

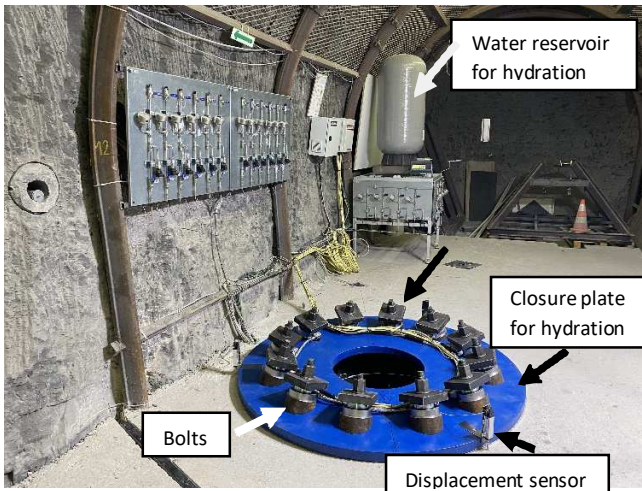


Fig. 14. General view of VSEAL 1 in situ test with the closure plate, bolts, load cells, displacement sensors and water reservoir.

Table 2. Sensor types and numbers.

Sensor type	Commercial name	Number
Relative humidity	Adapted Sensirion DHT75 model	6
Pore pressure	KELLER PA23SY	36
Water content	DELTAML3 TheraProbe	6
Total pressure cells	EARTHSYSTEM CP-02-TO-10-R	13
Load cell	SISGEO model 0L205V0500T	12
Displacement	ATEK LTM-50-A	3

5. Installation

VSEAL 1 main vertical borehole were drilled in September 2019 using an innovative patented drilling method. A special tower drill rig with 1 m single core barrel were used which provided very smooth wall and an extremely limited damaged zone (Fig. 15a and b). More details on the drilling method could be found in Cabrera Nunez (2013 and 2021). The final diameter was 1.005 m and the final depth ranged from 9.43 and 9.6 m due to the rock bedding.

Despite of the effort made to minimize perturbations of the rock during excavation, due to the long interruption period of the installation (one year), a damaged zone was developed around the shaft (Fig. 15c). These fissures were induced by desaturation and redistribution of stress state around the sidewalls. The induced damaged zone was carefully mapped before starting the bentonite core installation.

To drive the gas lines and cables to the bottom lid, an inclined borehole was drilled at an angle 45°. The borehole has a diameter of 0.101 m with no lining and a length of 14.2 m. It is connected to the main vertical borehole at a depth of 9.295 m (Fig. 16).

In addition, two vertical boreholes were drilled one at each side of the main shaft at 1.5 m from the wall, to drive the cables and the core instrumentation (Fig. 3). The diameter of those boreholes was 0.101 m with no lining. The borehole depths were 9 m and 8.4 m. The vertical boreholes were intersected with five sub-horizontal boreholes with an inner diameter of 0.046 m. They were drilled inclined upwards 24° from inside of the shaft to drive the cables from the shaft walls towards the vertical boreholes (Figs. 13a and 16). The drilling operations ended with levelling of the bottom face of the main shaft by a resin-based cement over 0.17 m.

The installation of VSEAL 1 started on September 2020, one year after the boreholes drilling. The first installation operation involved the descent of the bottom lid into the main shaft and passing of the cables and gas injection lines along the inclined borehole (Fig. 17a). The second step implicated grooving the shaft walls to house the rock sensors and WSR units and passing the cables through the sub-horizontal boreholes (Fig. 17b). The gaps around the sensors and the WSR units and cables have been done as narrow as possible and filled up with chemical anchorage leaving only the active parts of the sensors uncovered (Fig. 13b).



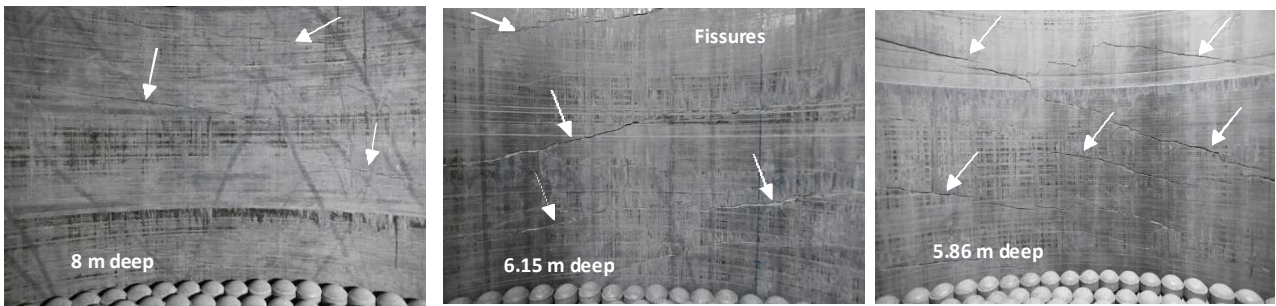


Fig. 15. (a) Tower drill rig with 1 m single core barrel, (b) View of VSEAL 1 main borehole with a diameter of ~1 m and a depth of ~9.6 m upon excavation, and (c) View of the sidewalls of the main borehole one year after excavation at different depths.

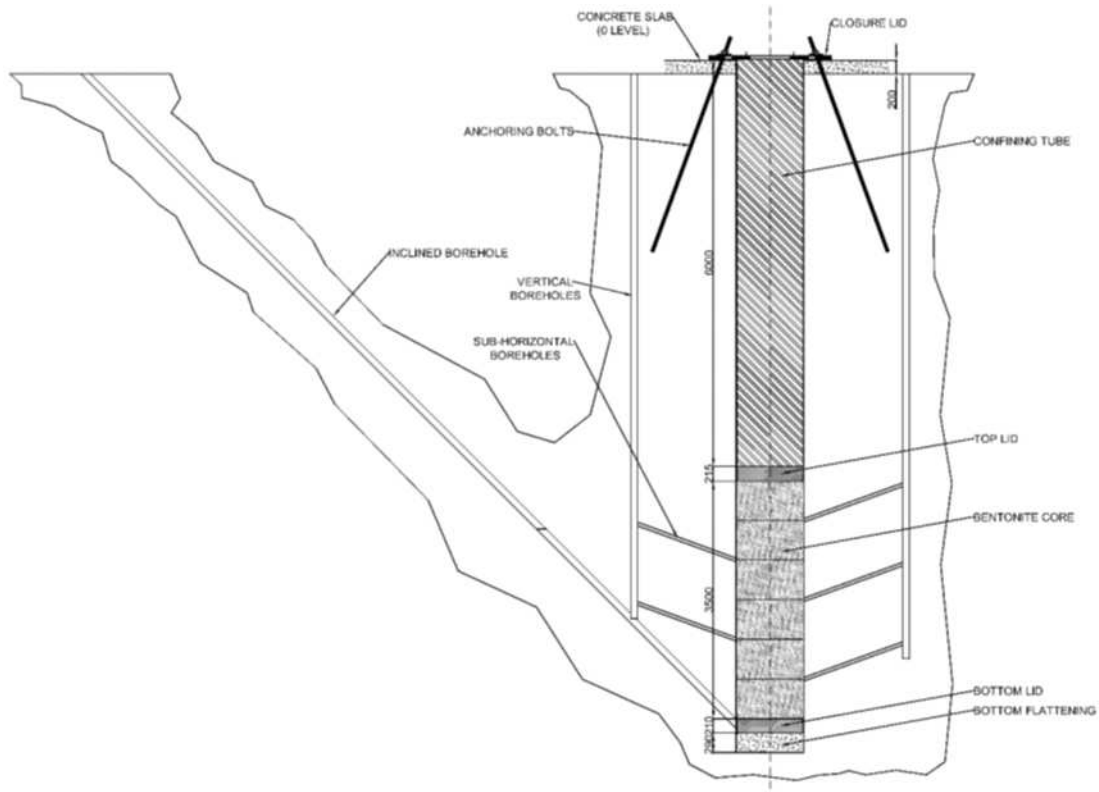


Fig. 16. Layout of boreholes and confining system (unit: ??).

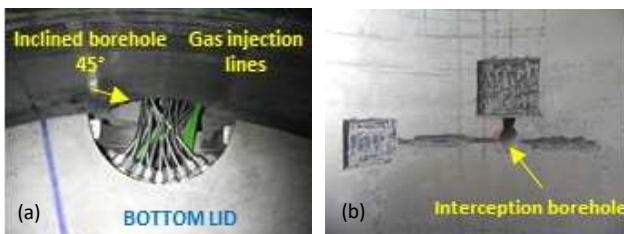


Fig. 17. (a) Bottom lid with gas connection lines passing through the inclined borehole, and (b) Grooves for sensors and WSR placement at shaft wall.

After connecting the sensors and checking they are functioning, the lateral (sub-horizontal, vertical, inclined) boreholes have been sealed to prevent leakage.

The main installation operation consisted in the building of the bentonite core with a diameter of 1 m and a length of 3.5 m (1/10 VSS) composed of MX80 bentonite pellet and powder mixture (80/20 in dry mass) at a target dry density of 1.49 Mg/m³. A special preparation protocol, consisting in placing manually the mixture layer-by-layer, was adopted. Molinero et al. (2017) tested three protocols to prepare

MX80 bentonite pellet and powder mixture (80/20 in dry mass) samples. The target dry density ($\rho_d = 1.49 \text{ Mg/m}^3$) was obtained with the layer-by-layer protocol only. The homogeneity of the specimens obtained by using each of the three protocols was examined by using X-ray computed microtomography. The results have shown that the layer-by-layer construction protocol provided a reasonably good homogeneity of the mixture, with regular scattering of the powder grains within the pores located between the pellets.

The bentonite core building comprised the emplacement of up to 120 layers of bentonite mixture starting of the upper face of the bottom lid. For each layer, the bentonite was arranged according to an ideal concentric arrangement and then gaps were filled by pouring manually the corresponding bentonite powder mass (20% in dry mass) (Fig. 18). Each level consisted of 750 pellets.

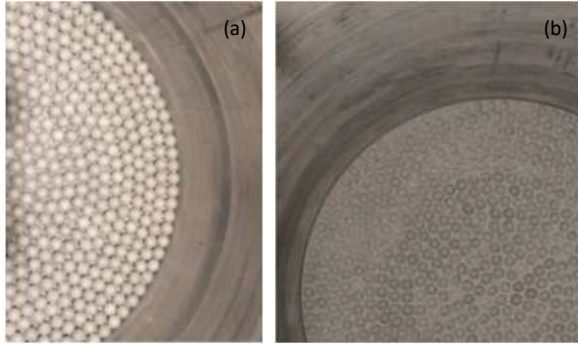


Fig. 18. (a) Pellets arrangement by layer, and (b) Results after pouring the bentonite powder.

Despite of trying to reduce initial structural heterogeneities, several defects occurred during the in situ installation process. Indeed, a technological gap remained at the upper zone between the last mixture layer (Layer 120) and the top lid. The gap has a varied thickness and a convex form (Fig. 19). The calculated gap volume is ~ 9 L.

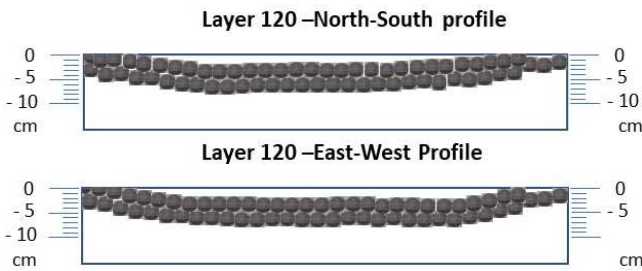


Fig. 19. Profiles and thickness of the top technological gap existing between the top layer of pellets and the top lid.

During the installation process, it was observed that, for some layers, the powder was not homogeneously distributed with some inter-pellet voids remaining unfilled (Fig. 20) at different zones and especially close to the bentonite-rock interface. Alcantara et al. (2020) determined the volumetric degree of the powder filling of the binary mixture (MX80 bentonite/pellet and powder) prepared following the layer-by-layer protocol at the same dry density as $F = \rho_{d, \text{powder}}^{\text{min}} / \rho_{d, \text{powder}}$, where $\rho_{d, \text{powder}}^{\text{min}}$ is the minimum dry density of the powder with a mass fraction of 20% and $\rho_{d, \text{powder}}$ is the powder dry density. For the bentonite core in VSEAL 1, the calculated value is $F = 0.47$ which corresponds to an under filled pellets packing supported structure according to Vallejo (2001)'s classification. For the bulk volume of the powder to fill completely the inter-pellet voids, the minimum powder proportion (PP) can be calculated as defined by

Vallejo (2001) and de Frias Lopez et al. (2016) as $PP = [\varphi_{\text{pellets}} (1 - \varphi_{\text{powder}})] / [\varphi_{\text{pellets}} (1 - \varphi_{\text{powder}}) + (1 - \varphi_{\text{pellet}})]$, where φ_{pellets} is the porosity of a sample composed of a packing of pellets (without powder) and φ_{powder} is the porosity of the poured powder filling the same volume. For the mixture used in VSEAL 1, the measured dry density of the pellets packing is $\rho_{d, \text{pellets}} = 1.18 \text{ Mg/m}^3$ ($\varphi_{\text{pellets}} = 0.57$) and the dry density of the powder is estimated to $\rho_{d, \text{powder}} = 1.1 \text{ Mg/m}^3$ ($\varphi_{\text{powder}} = 0.59$) which leads to a minimum powder proportion $PP = 24\%$. For the bentonite core in Vseal 1 in situ test, the unfilled inter-pellets voids observed at some layers might be due to the low powder proportion as compared to the PP value combined to the adopted pouring methods (manual pouring) which is operator-dependent (most of the unfilled inter-pellets void are located at the periphery of bentonite layer, which is difficult to fill manually).

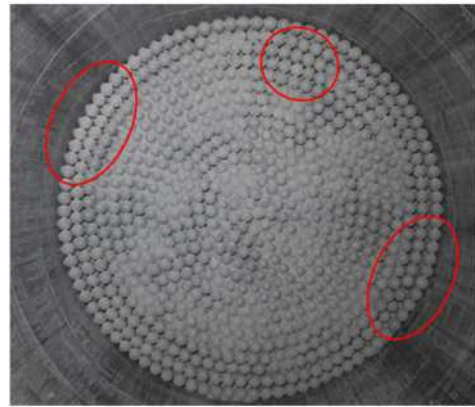


Fig. 20. View of Layer 117 with heterogenous distribution of the bentonite powder.

As the bentonite core construction is progressing the sensors with the data transmitter were installed at the planned instrumented layer (Fig. 21). Each instrumentation set-up consisted of a WSE unit, and six sensors (two pore pressure, two relative humidity and two water content sensors). The set-up was distributed on the mixture layer according to the layout given in Figs. 11 and 21. After placing the set-up, the remaining pellets were arranged to complete the layer and finally the bentonite powder was poured on.

The final operation step comprised emplacement of the top lid and the confining system (confining tube and closure plate). A soft rubber O-ring was placed on the periphery within the 0.002 m gap left between the top lid and the shaft walls. It was then filled up with a sealing resin to prevent any leakage. Once the confining metal tube installed, the gap around it was also filled up with a sealing resin.

The installation of VSEAL 1 was completed in August 2021. The hydration phase started in October 2021. The water used has the same salinity as the pore water of the Callovo-Oxfordian claystone from Meuse/Haute-Marne URL in France.

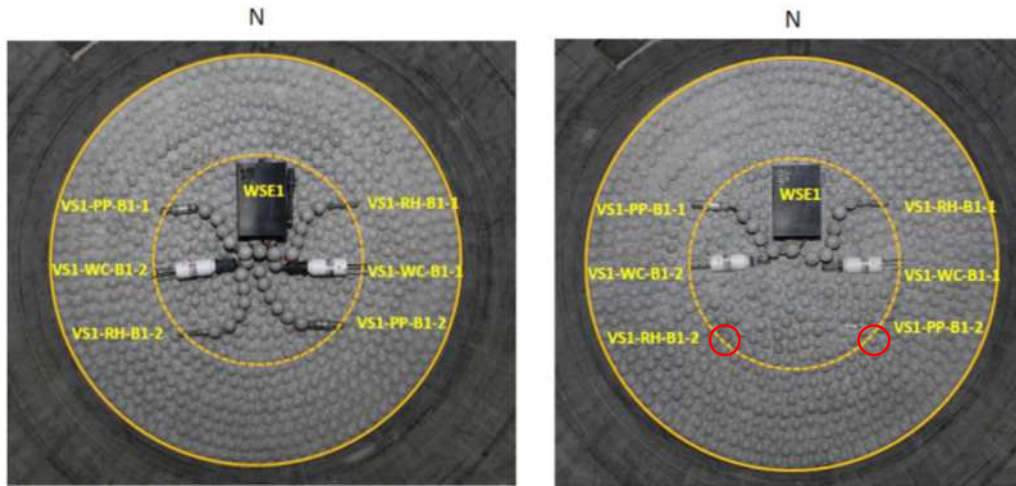


Fig. 21. Arrangement of sensors in Layers 10 (left) and 11 (right) for instrumented set-up installed at 8.9 m depth (section B1). VS1 refers to VSEAL 1 test.

6. Results and discussion

The hydration phase started by opening the water tank valves. No water pressure was applied. The measured water inflow over time is shown in Fig. 22. Once hydration started, the water volume increased rapidly and reached 30.5 L in a few hours, filling notably the upper technological gap. However, the injection was stopped for two weeks due to a technical problem related to the water leakage of the system. Note that the initial injected volume is higher than the volume of the top convex gap (9 L), suggesting the existence of additional technological gaps and preferential flow paths where some water infiltration could have occurred. Upon restart of hydration, the water intake slowed down to a very low rate and reached 42 L after 334 d. The observed decrease of the water injection rate might be induced by the swelling of the upper layer of the bentonite core during the shutting week, and the reduction of the bentonite buffer permeability at this zone.

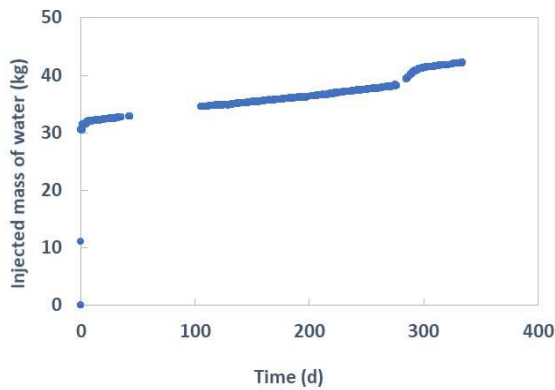


Fig. 22. Injected mass of water versus time.

Six relative humidity and water content sensors were installed in the bentonite core at three sections named B1, B2 and B3 located at 0.318 m, 0.198 m and 0.028 m respectively from the hydration face (top lid). Variations with time of *RH* measured at different sections are displayed in Fig. 23a. No data are registered between 70 d and 133 d due to a temporary problem in the data acquisition system (DAS) units. Once the hydration started, a monotonic increase of *RH* is observed at sensors RH-B3-1 and RH-B3-2 located at 28 cm from the hydration

front. After 340 d, *RH* values ranged between 55% and 58%, with the initial value being 50%. A slight increase of relative humidity is also observed at sensors RH-B2-1 and RH-B2-2 located at the central zone of the bentonite core. At this zone, hydration of the mixture is probably driven by vapor transfer from the hydrated zone (outer layers) to the dry center of the bentonite core. As expected, no change of *RH* at sensors located at 32 cm from the bottom lid (3.18 m from the top lid) is observed.

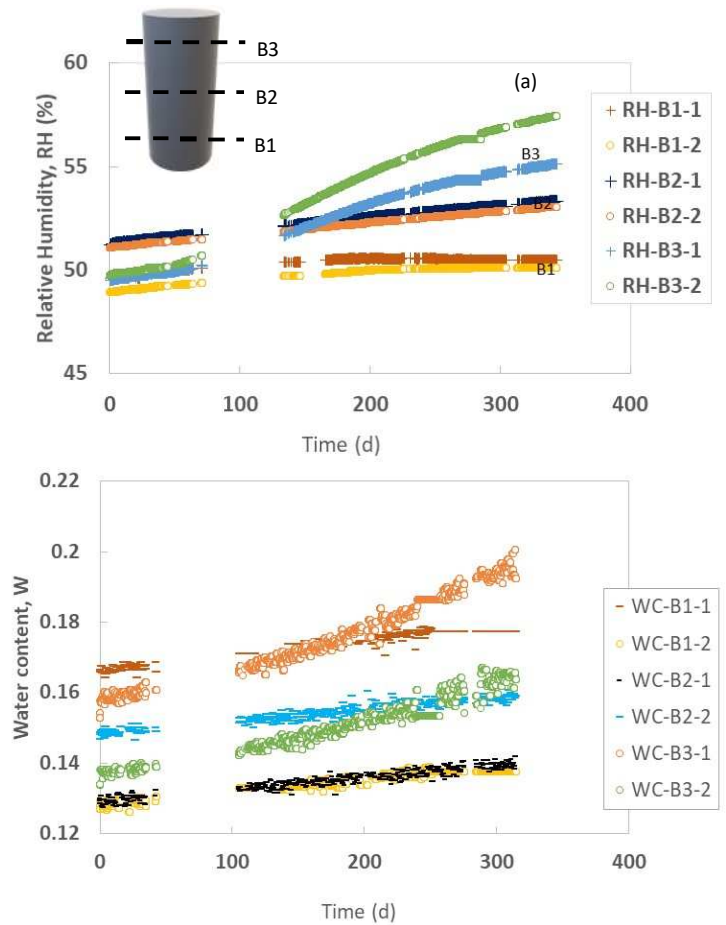


Fig. 23. *RH* (a) and *w* (b) evolution measured at different distances from the top hydration source.

Variation of water content (W) measured at different depths are shown in Fig. 23b. A slow increase of W is observed at the sensors located at 28 cm from the top lid, consistent with RH evolution at the same location. The variation ranged between 2.7% and 4.7% after 314 d. No significant increase of W is measured at sections B1 and B2 located further from the hydration face. Indeed, after 314 d, the measured variation at these locations is around 1%. Fig. 24 shows the suction profiles after 50 d and 340 d obtained by plotting mean suction values at sensors RH- i - j ($i = 1, 2, 3; j = 1, 2$). Total suction is related to RH via the psychrometric (Kelvin's) equation, $H = \exp\{sM_w/[R(273 + T)\rho_l]\}$, where M_w is the molecular weight of water, T is the temperature in Celsius, R is the gas constant, ρ_l is the liquid density, and s is the suction. Initial suction values range between 89 MPa and 94 MPa. The overall evolution of the curves shows a slow decrease of suction due to the saturation progress with lower suction values at short distance from the top hydration source as time increases.

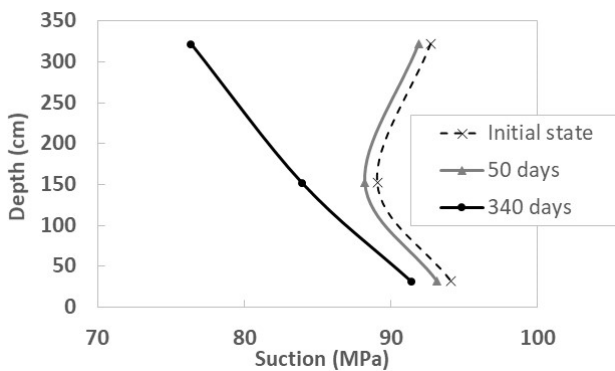


Fig. 24. Profiles of suction after 0 d, 50 d and 340 d of hydration measured at different depths of the clay core.

During hydration, both axial and radial swelling pressures are monitored using 13 load cells (Figs. 9, 13 and 19). Fig. 25 shows the axial swelling pressure measured at four load cells located at the top lid. Upon hydration, a slow increase of swelling pressure is observed at the four locations. After 130 d, the measured values ranged between 0.9 bar and 3.15 bar. As for RH measurement, no data are registered between 70 d and 133 d due to a temporary problem in the DAS units. In addition, a malfunctioning is observed at sensors TP-BT2, TP-BT3 and TP-BT4 where a sudden decrease in pressure to negative values is observed upon fixing of the DAS units (at day 108) and one month later at sensor TP-BT2. More investigation is needed to determine the malfunctioning causes of the sensors. The registered low values are probably due to the existence of the convex technological gap. Indeed, the hydro-mechanical behavior of the sealing mixture is first characterized by free swelling conditions because of the progressive filling of the technological gap. A rebuild up of the swelling pressure may be expected upon recovery of constant volume conditions and further hydration of partially saturated regions.

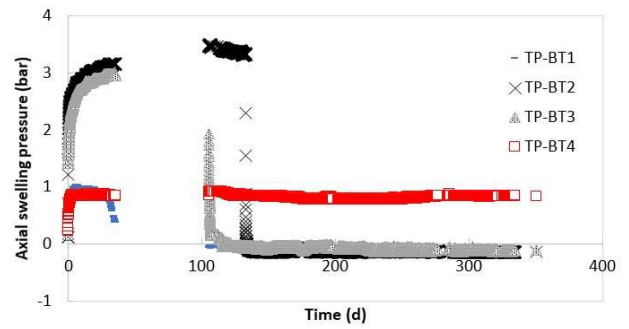


Fig. 25. Evolution of axial swelling pressure measured at top lid.

The evolution of axial swelling pressure measured at the bottom lid located at 3.5 m from the hydration front is shown in Fig. 26. Surprisingly, upon hydration, the swelling pressure increased at sensor TP-BB2 with a constant rate till reaching 4.9 bar after 340 d. This unexpected result can be attributed to the existence of damaged area with interconnected fissures crossing the shaft wall where some water infiltration could have occurred inducing some local swelling at the bottom layer of the bentonite mixture. A view of the shaft wall in the vicinity of this sensor is shown in Fig. 27. No significant increase in axial swelling pressure is observed at sensors TP-BB1, TP-BB3 and TP-BB4, suggesting that the interconnected fissures along the shaft wall were more developed in the vicinity of sensor TP-BB2 (Fig. 27).

Moreover, due to the induced installation defects, some water infiltration through the bentonite core-rock interface might have occurred, inducing radial hydration of the mixture. This hypothesis is corroborated when observing the evolution of radial swelling pressure at different depths along the shaft wall (Fig. 28). A monotonic increase of swelling pressure is observed at sensors TP-R1, TP-R2, TP-R3, TP-R4 and TP-R5 located at 290 cm, 231 cm, 173 cm, 114 cm and 56 cm, respectively, from the top lid (hydration face). The reached value after 280 d ranges between 1.5 bar and 2.5 bar.

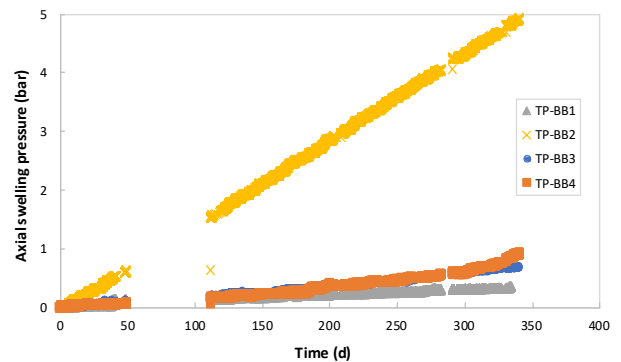


Fig. 26. Evolution of axial swelling pressure measured at bottom lid.

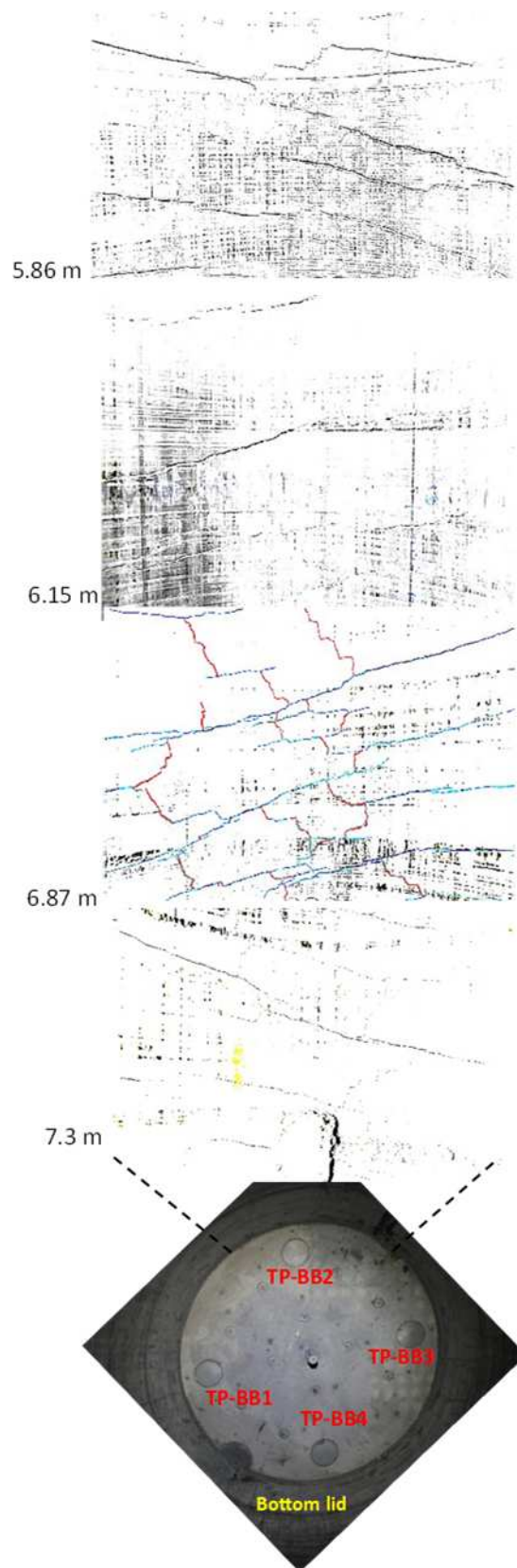


Fig. 27. View of the shaft wall with interconnected fissures in the vicinity of sensor TP-BB2.

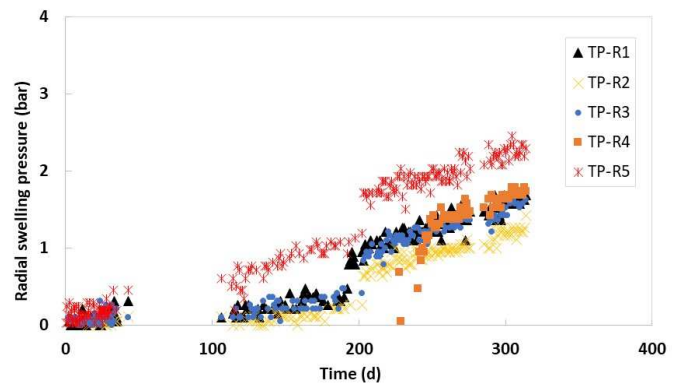


Fig. 28. Evolution of radial swelling pressure measured at the bentonite-rock interface at five sections located at different depth.

7. Concluding remarks

In the framework of VSEAL project, a large-scale vertical sealing test VSEAL 1 have been installed in Tournemire URL to investigate the the impact of gas migration on the long-term performance of bentonite-based VSS. The swelling core consisted of MX80 bentonite pellet and powder mixture (80/20 in dry mass). A specific protocol was adopted to construct the bentonite seal in order to minimize as much as possible initial structural heterogeneities induced by the installation process and to reach the target dry density of 1.49 Mg/m^3 . The in situ test was equipped of wireless sensors within the bentonite core and wired sensors at the bentonite-rock interface. To the best of the authors' knowledge, VSEAL 1 is the unique in situ sealing test with a well-known initial structural distribution of the pellets and the powder within the tested mixture. Although some heterogeneities occurred during the installation, an extra effort was made to characterize and localize these zones. The knowledge of the initial structural distribution of is valuable for analysis of the results, especially during the gas injection phase and for future numerical modeling A first analysis of the results during the hydration phase in terms of injected water volume, relative humidity, water content and swelling pressures (axial and radial) allowed the following conclusions to be drawn:

- (1) Upon hydration, a large volume of water was injected rapidly due to the existence of a convex technological gap between the last pellet layer and the top lid. Furthermore, interconnected fissures located at the shaft wall favored some water infiltration towards the bottom layer of the mixture. In addition, the presence of installation-induced structural heterogeneities (non-homogenous distribution of the powder) at the bentonite-rock interface might have constituted preferential flow paths and favored local radial hydration of the bentonite core. During the saturation process, the evolution of RH and W within the mixture fitted well for a given hydration distance.
- (2) The existence of additional infiltration paths influenced greatly the evolution of axial and radial swelling pressures, since they induced the simultaneous top, radial and bottom local hydration of the core resulting of an unexpected local increase of swelling pressure in a zone located very far from the top hydration face.
- (3) VSEAL 1 early testing results show that under geological disposal conditions, the existence of even a limited damaged zone at the shaft wall, in addition to the unavoidable technological voids

remaining after construction of the bentonite-based core, allows water to reach, at an early-stage, the bottom zones of the VSS, promoting early saturation of the bottom layers. In this situation, when gas reaches the VSS, the bottom layer might be saturated like the top layer which will probably influence the subsequent behavior of the VSS. The impact of this behavior on the long-term performance of the VSS under gas loading remains to be studied.

- (4) The installation-induced heterogeneous distribution of the mixture might lead to remaining dry density gradients after full saturation which, thanks to the accurate records made during the installation, could be considered during the gas injection phase and in the evaluation of long-term performance of VSS.

Declaration of competing interest

The authors declare that they have no known competing financial interests or personal relationships that could have appeared to influence the work reported in this paper.

References

- Alcantara, A.M., Romero, E., Mokni, N., Olivella, S., 2020. Microstructural and hydro-mechanical behavior of bentonite pellets and powder mixture. *E3S Web Conf.* 195, 04003.
- Andra, 2016. Safety options report - Post-closure part (DOS-AF). Technical Report No. CG-TE-NTE-AMOA-SR2-0000-15-0062. Andra.
- Andra, 2021. Dossier d'enquête publique préalable à la déclaration d'utilité publique du centre de stockage Cigéo. Piece No. 4 caractéristiques des ouvrages les plus importants (in French).
- Cabrera Nunez, J., 2013. Procédé et dispositif de forage non destructif. Brevet français No. FR 2974141-B1. Institut de Radioprotection et de Sureté Nudéaire (in French).
- Cabrera Nunez, J., 2021. Procédé et dispositif de forage grand diamètre ou de creusement de puits suivant plusieurs inclinaisons. Brevet français No. FR 3100559-B1. Institut de radioprotection et de sureté nucléaire (in French).
- Carbonell, B., Villar, M.V., Martín, P.L., Gutiérrez-Álvarez, C., 2019. Gas transport in compacted bentonite after 18 years under barrier conditions. *Geomech. Energy Environ.* 17, 66-74.
- Cuss, R.J., Harrington, J.F., Graham, C.C., Noy, D.J., 2014. Observations of pore pressure in clay-rich materials; implications for the concept of effective stress applied to unconventional hydrocarbons. *Energy Procedia* 59, 59-66.
- Cuss, R.J., Harrington, J.F., Noy, D.J., 2010. Large scale gas injection test (Lasgit) performed at the Äspö Hard Rock Laboratory. Technical Report TR-10-38. Svensk Kärnbränsle hantering AB (SKB), Stockholm, Sweden.
- De Frias Lopez, R., Silfwerbrand, J., Jelagin, D., Birgisson, B., 2016. Force transmission and soil fabric of binary granular mixture. *Geotechnique* 66 (7), 578-583.
- De La Vaissière, R., Armand G., Talandier J., 2015. Gas and water flow in an excavation-induced fracture network around an underground drift: A case study for a radioactive waste repository in clay rock. *J. Hydrol.* 521, 141-156.
- De La Vaissière, R., Gerard, P., Radu, J.P., et al., 2014. Gas injection test in the Callovo-Oxfordian claystone: Data analysis and numerical modelling. *Geol. Soc. Lond., Spec. Publ.* 400, 427-441.
- DOPAS, 2016. Test report on FSS metric clayish material emplacement tests with clayish material definition and laboratory work on its performance. Deliverable D3.7. Andra.
- FORGE, 2014. WP5 final report: Experiments and modelling of gas migration processes in undisturbed rocks. Technical Report D5.19-VER. 1.0. FORGE.
- Gens, A., Vallejan, B., Sánchez, M., Imbert, C., Villar, M.V., VanGeet, M., 2011. Hydro-mechanical behaviour of a heterogeneous compacted soil: experimental observations and modelling. *Géotechnique* 6, 367-386.
- Graham C., Harrington, J.F., Sellin, P., 2016. Gas migration in pre-compacted bentonite under elevated pore-water pressure conditions. *Appl. Clay Sci.* 132-133, 353-365.
- Graham, C.C., Harrington, J.F., Cuss, R.J., Sellin, P., 2014. Pore-pressure cycling experiments on Mx80 Bentonite. *Geol. Soc. Lond. Spec. Publ.* 400 (1), 303-312.
- Gutiérrez-Rodrigo, V., Pedro Luis Martín, P.L., Villar, M.V., 2021. Effect of interfaces on gas breakthrough pressure in compacted bentonite used as engineered barrier for radioactive waste disposal. *Process Saf. Environ. Protect.* 149, 244-257.
- Harrington, J.F., Dela Vissiere, R., Noy, D.J., Cuss, R.J., Talandier, J., 2012b. Gas flow in Callovo-Oxfordian claystone (Cox): Results from laboratory and field measurements. *Mineral. Mag.* 76, 3303-3318.
- Harrington, J.F., Horseman, S.T., 2003. Gas migration in KBS-3 buffer bentonite: Sensitivity of test parameters to experimental boundary conditions. Report TR-03-02. Svensk Kärnbränslehantering AB (SKB), Stockholm, Sweden.
- Harrington, J.F., Milodowski, A.E., Graham, C.C., Rushton, J.C., Cuss, R.J., 2012a. Evidence for gas induced pathways in clay using a nanoparticle injection technique. *Mineral. Mag.* 76, 3327-3336.
- Harrington, J.F., Graham, C., Cuss, R., Norris, S., 2017. Gas network development in a pre-compacted bentonite experiment: Evidence of generation and evolution. *Appl. Clay Sci.* 147, 80-89.
- Horseman, S.T., Harrington, J.F., Sellin, P., 1997. Gas migration in Mx80 buffer bentonite. In: Gray, W.J., Triay, I.R. (Eds.), *Proceedings of the Scientific Basis for Nuclear Waste Management XX*. Materials Research Society, Warrendale, Pennsylvania, USA. pp. 1003-1010.
- Horseman, S.T., Harrington, J.F., Sellin, P., 1999. Gas migration in clay barriers. *Eng. Geol.* 54, 139-149.
- Mokni, N., Barnichon, J.D., Dick, P., Nguyen, T.S., 2016a. Effect of technological macro voids on the performance of compacted bentonite/sand seals for deep geological repositories. *Int. J. Rock Mech. Min. Sci.* 88, 87-97.
- Mokni, N., Molinero Guerra, A., Cui, Y.J., et al., 2019. Modelling of the long term hydromechanical behavior of a bentonite pellet/powder mixture with the consideration of initial heterogeneities. *Geotechnique* 70, 563-580.
- Mokni, N., Barnichon, J.D., 2016b. Hydro-mechanical analysis of SEALEX in situ tests - Impact of technological gaps on long term performance on repository seals. *Eng. Geol.* 205, 81-92.
- Molinero-Guerra, A., Mokni, N., Delage, P., et al., 2017. In depth characterisation of a mixture composed of powder/pellets MX80 bentonite. *Appl. Clay Sci.* 135, 538-546.
- Molinero-Guerra, A., Aïmedieu, P., Bornert, M., et al., 2018. Analysis of the structural changes of a pellet/powder bentonite mixture upon wetting by X-ray computed microtomography. *Appl. Clay Sci.* 165, 164-169.
- Molinero-Guerra, A., Cui Y.J., He, Y., et al., 2019. Characterization of water retention, compressibility and swelling properties of a pellet/powder bentonite mixture. *Eng. Geol.* 248, 14-21.
- Namiki, K., Hidekazu Asano, H., Takahashi, S., Shimura, T., Hirota, K., 2014. Laboratory gas injection tests of compacted bentonite buffer material for TRU waste disposal. *Geol. Soc. Lond., Spec. Publ.* 400, 521-529.
- Pusch, R., 1979. Mineral-water interactions and their influence on the physical behavior of highly compacted Na bentonite. *Can. Geotech. J.* 19, 381-387.
- IRSN, 2014. Projet de stockage Cigéo Ouvrages de fermeture. Technical Report No. 2014-00006. IRSN.
- Saba, S., Delage, P., Lenoir, N., Cui, Y.J., Tang, A.M., Barnichon, J.D., 2014. Further insight into the microstructure of compacted bentonite/sand mixture. *Eng. Geol.* 168, 141-148.
- Sellin, P., Harrington, J.F., 2006. Large-scale gas injection test (Lasgit) current status. In: *American Nuclear Society High Level Waste Meeting*, Las Vegas.
- Troulino, I., Verstricht, J., 2015. The PRACLAY seal gas-injection experiments. Report No. ER-291. SCK-CEN.
- Vallejo, L.E., 2011. Interpretation of the limits in shear strength in binary granular mixtures. *Can. Geotech. J.* 38 (5), 1097-1104.

- Villar, M.V., Lloret, A., 2008. Influence of dry density and water content on the swelling of a compacted bentonite. *Appl. Clay Sci.* 39, 38-49.
- Villar, M.V., Martín, P.L., Romero, F.J., Barcala, J.M., Gutiérrez-Rodrigo, V., 2012a. Gas transport through bentonite: Influence of dry density, water content and boundary conditions in: *Propriétés de Transfert des Géomatériaux. Transfert*, 379-389. (F. Skoczylas, C.A. Davy, F. Agostini, and N. Burlion, editors). *Transfert 2012, Actes du Colloque*
- Villar, M.V., Martín, P.L., Bárcena, I., García-Siñeriz, J.L., Gómez-Espina, R., Lloret, A., 2012b. Long-term experimental evidences of saturation of compacted bentonite under repository conditions. *Eng. Geol.* 149-150, 57-69.
- Vomvoris, S., Marschal, P., Kickmaier, W., 2011. GMT - A large scale in-situ test of the gas migration properties of engineered barriers. *MRS Online Proceedings Library* 663, 553.
- Wang, Q., Tang, A.M., Cui, Y.J., Delage, P., Barnichon, J.D., Ye, W.M., 2014. The effects of technological voids on the hydro-mechanical behaviour of compacted bentonite sand mixture. *Soils Found.* 53, 232-245.
- Yong, R.N., Boonsinsuk, P., Wong, G., 1986. Formulation of backfill material for a nuclear fuel waste disposal vault. *Can. Geotech. J.* 23, 216-228.



Nadia Mokni obtained his MSc degrees in Civil Engineering from National School of Engineering of Tunis (Tunisia), in 2006, and her PhD in Geomechanics from polytechnic University of Catalonia, in 2011. She has been leading the Geomechanics Research area at the French Institute for Radiological Protection and Nuclear Safety since 2013. Her research interests include (1) experimental investigations on the chemo-hydro-mechanical (CHM) behaviors of bentonite-based engineered barriers for deep geological disposal of nuclear waste and host rocks (clay); and (2) numerical modeling of coupled THMC processes in clays. She has been participated in a large number of European projects.